06

Thermally initiated modification of the structure and magnetic properties of Ta/Ni and FeMn/Ni film nanocomposites

© V.O. Vas'kovskiy,[1,2] A.A. Bykova,[1] A.N. Gorkovenko,[1] N.A. Kulesh,[1] V.N. Lepalovskij,[1] E.V. Kudyukov,[1] N.V. Selezneva[1]

[1] Ural Federal University after the first President of Russia B.N. Yeltsin, Yekaterinburg, Russia
[2] M.N. Mikheev Institute of Metal Physics, Ural Branch, Russian Academy of Sciences, Yekaterinburg, Russia
e-mail: a.n.gorkovenko@urfu.ru

Received October 4, 2024
Revised February 17, 2025
Accepted February 17, 2025

The effect of thermomagnetic treatment on the structure and magnetic properties of films containing Ni layers in the vicinity of Ta layers or antiferromagnetic FeMn layer has been studied. It is shown that annealing at temperatures up to 300 °C significantly affects the nature of induced anisotropy in the ferromagnetic layer, which leads to variations in the anisotropy of the coercive force in Ta/Ni films or the anisotropy of the exchange bias field in FeMn/Ni films. Annealing at a higher temperature causes uneven interlayer diffusion of elements, which, according to profile X-ray fluorescence analysis, extends to a depth of at least 5 nm. This is accompanied by a sharp increase in the coercive force for Ta/Ni films and an increase in the resulting magnetization for FeMn/Ni films while maintaining the effect of exchange bias in them.

Keywords: annealing, exchange bias, diffusion, anisotropy, antiferromagnetic.

DOI: 10.61011/TP.2025.06.61376.311-24

Introduction

Multilayer magnetic films are among the functional media that have been used in real technical applications thus leading to high interest of researchers in the technology and physics of such materials [1]. Among them, high position is held by the ferromagnetic/antiferromagnetic composites, on the basis of which the spin valves, MRAM memory elements and other magnetic sensor and spintronic devices are constructed [2–4]. If composites incorporate an antiferromagnetic layer provided there's an interlayer exchange interaction it results in the so-called magnetic (exchange) bias, which ensures stabilization of a homogeneous magnetic structure in the ferromagnetic layer. Naturally, in order to effectively ensure its function, the temperature of an antiferromagnet in the film state shall not exceed the room temperature. This antiferromagnets potentially include a whole number of Mn-based alloys. Despite the fact that α-Mn, which at room temperature is in equilibrium state, does not satisfy this condition, it can form a highly stable antiferromagnetic structure in alloys. The most well-known binary systems exhibiting high-temperature antiferromagnetism in the film state include Ir−Mn, Pt−Mn, Pd−Mn, Ni−Mn, Cr−Mn, Fe−Mn [5,6]. To date, it is the layers of Ir−Mn that are part of the critical elements of spintronics [7]. Moreover, Mn alloy films with other platinum group metals manifest high functional properties, providing the necessary level and good temperature stability of hysteresis in adjacent ferromagnetic layers. At the same time, because of economic reasons there's a niche for the use of less expensive antiferromagnetic alloys, e.g., FeMn [8]. The only drawback of this antiferromagnet is the relatively low Neel temperature (~ 500 K), which leads to increased temperature sensitivity of the film structures based on it, which, however, can be controlled using hardware.

Antiferromagnetism of Mn in binary alloys provides both the functionality of precision technical elements and the ability to optimize their properties for specific tasks. At the same time, it is known that in Mn-containing film structures, when heated to relatively low temperatures, irreversible degradation of the initial magnetic properties is observed, which is primarily associated with an increased tendency of Mn to migrate from the volume of „its own" layer to the surface or adjacent layers not containing Mn. Such a generalized conclusion follows from the findings of a number of studies devoted to this issue on films with a large number of layers that are close to real spin-valve media [9–14], or on their somewhat simplified analogues [15,16]. They indicate, among other things, the predominant migration of Mn along grain boundaries, as well as along the oxygen gradient and variation of the latter due to the introduction of a barrier oxide layer. In most cases, information about the elements thickness profiles was obtained using ion etching of films by secondary ion mass spectrometry (SIMS) [11,13], photoelectron spectroscopy (XPS) [14] or Auger spectroscopy (AFS) [14,15], and describes the results of single annealing.

The present study is considered as a continuation of this kind of research in order to obtain a more detailed and systematic information on the relationship of macroscopic magnetic properties with structural and compositional changes in Mn-containing multilayer systems under varying thermal conditions. For this purpose, relatively simple

objects based on FeMn/Ni bilayers and a non-destructive technique for profile analysis of the elemental composition were selected — X-ray fluorescence spectroscopy on full internal reflection. This version of the layered structure is considered primarily as a model, which predetermined the choice of its components. On the one hand, it does not contain single elements in different layers, on the other hand, it has the simplest possible total elemental composition, and, finally, the antiferromagnetic state is relatively simple to realize in FeMn alloy films. At the same time, such a structure may also be of independent practical interest as a strain-magnetoresistive medium. It is known that Ni has significant negative magnetostriction and magnetoresistance anotropy, which are the defining characteristics of these media, but this combination is optimally realized in a structure with a magnetic bias [17].

1. Technology aspects

To comprehensively solve this problem, film samples with a layered structure of three types were studied glass/Ta(5)/Ni(40)/Ta(5), glass/Ta(5)/$Fe_{20}Ni_{80}$(5)/FeMn(20)/Ni(40)/Ta(5), Si/FeMn(5)/Ni(5). In the mentioned structural formulae the inclined lines denote lamination, and the digits in parentheses — thicknesses of layers in nm. All films were obtained by magnetron sputtering on Orion-8 system on Corning cover glasses or monocrystalline silicon wafers with the following general technological parameters: residual gas pressure $5 \cdot 10^{-7}$ mm · Hg; argon working gas pressure 10^{-3} mm · Hg; the presence of an electric bias on the substrate with a power of 14 W; the presence of a technological magnetic field with a strength of 250 Oe in the substrate plane. Targets made of pure materials or alloys, made in the form of two-inch discs, were used for sputtering. The thin Ta layers present in the two types of samples mainly served a protective function, but for a structure containing FeMn, the underlying Ta layer also served a structure-forming agent [8]. During the experiment, the films were subjected to cumulative stepwise annealing at temperatures from 200 to 400 °C. Annealing was carried out in vacuum at a pressure of residual gases $5 \cdot 10^{-7}$ mm · Hg and in the presence of a magnetic field aligned with the process field. Duration of each step was 1 h.

To achieve the objectives of the study, several variants of film structures were selected. Glass/Ta/Ni/ta films were considered as auxiliary films and were used to determine changes in the properties of Ni layer during annealing that were not related to the presence of an adjacent FeMn layer. The hard-melting layer of Ta was expected to interfere with the inter-layer diffusion, thus making it possible to study the properties of the isolated Ni layer. The films of glass/Ta/$Fe_{20}Ni_{80}$/FeMn/Ni/Ta were the main focus of the magnetic properties studies where the irreversible nature of these properties was examined during the work. It can be seen from the formula that they contain a thin layer of permalloy, the presence of which does not directly contribute to solving the problem. However, due to its epitaxial action, it makes it possible to fix in the equiatomic FeMn alloy a nonequilibrium FCC crystal structure at room temperature, in which the antiferromagnetic state is realized [18]. And, finally, Si/FeMn/Ni films were intended for direct examination of the elements thicknesses profile using the X-ray fluorescent analyzer Nanohunter. This device implements a technique for the complete external reflection of a gazing X-ray beam that penetrates the material to a depth of no more than 10−20 nm. This, in particular, is due to the absence of all auxiliary layered elements and the small thickness of the main layers in these samples. In addition, to eliminate the „clogging" effect of the elements present in the glass in the resulting fluorescence spectrum, the latter was replaced with monocrystalline silicon.

Along with the above-mentioned fluorescent analyzer, the stylus profilometer Dektak-150 and diffractometers Bruker D8 were used to certify films in thickness and structure, respectively. At that diffractometry was carried out for radiation CuK_α and in geometry „$\theta/2\theta$". Magnetic measurements were performed on vibration magnetometer Lakeshore.

2. Proving the presence of Ni layers in Ta/Ni/Ta films

By itself, Ni at room temperature is characterized by low spontaneous magnetization, relatively low four-axis crystalline anisotropy, and negative magnetostriction. Taken together, this creates the prerequisites for a wide variability of magnetic and other properties associated with the presence of magnetic ordering, depending on the conditions of films fabrication, substrate material, subsequent treatments, and the presence of conjugated layers [19]. Figure 1 shows diffractograms characterizing the structure of Ta/Ni/Ta sample at different stages of annealing. (Hereafter, the presence of a glass substrate is not specified in the structural formula, but it is present as the first (left) constituent element). They have a single diffraction line, indicating the presence in the polycrystalline layer of Ni of a strong crystalline texture (111), i.e., a predominant orientation of the atomic planes (111) parallel to the plane of the films, regardless of the intensity of thermal effect. The presence of Ta layers is not shown on diffractograms, most likely due to the low thickness and high dispersion of the structure. Literary sources [20] indicate the typical nature of this kind of the grain-oriented structure for films with a FCC structure deposited on Ta. To this in accordance with Fig. 1 it is possible to add a conclusion about its high stability, which, apparently, is inherited from the Ta buffer layer, which plays a key role in this texture formation.

The table below gives some qualitative data characterizing the structure of the studied sample, namely average sizes of crystallites D, found from Scherer formula [21], and the distances h between the atomic planes like (111) calculated using FullProf Suite software [22]. Based on

The average crystallite size, determined by the Scherer formula [21], and the interplanar spacing (111) for Ni and FeMn layers in two types of samples after thermomagnetic treatment at different annealing temperatures

Type of the film structure	glass/Ta/Ni/Ta		glass/Ta/$Fe_{20}Ni_{80}$/FeMn/Ni/Ta			
Layer composition	Ni		Ni		FeMn	
Parameters of the structure	D, nm	h, nm	D, nm	h, nm	D, nm	h, nm
As-deposited	20	0.2032	28	0.2026	19	0.2071
$T_a = 200\,^\circ$C	24	0.2027	29	0.2030	19	0.2078
$T_a = 300\,^\circ$C	25	0.2025	28	0.2028	19	0.2077
$T_a = 400\,^\circ$C	26	0.2022	32	0.2025	–	–

N o t e. Systematic errors in defining the given values D and h make ± 1 nm and ± 0.0001 nm respectively.

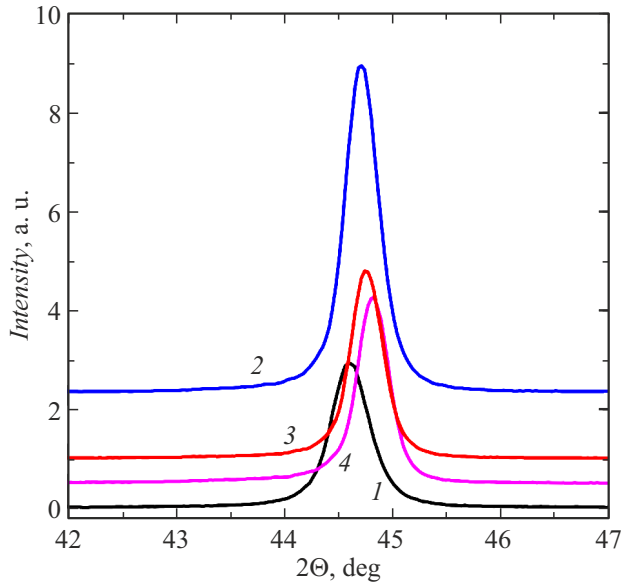

Figure 1. Diffractograms of Ta/Ni/Ta sample measured after annealing at various temperatures: *1* — initial state; *2* — 200 °C; *3* — 300 °C; *4* — 400 °C.

these data we may conclude that the film has a highly dispersant (nanocrystalline) structure. With the growth of T_a the value D has a tendency to growth. However, up to $T_a \leq 300\,^\circ$C this tendency is likely not to be the result of recrystallization, but rather reflects the relaxation of the elastic stresses and defects of the lattice. The behavior of parameter h during thermal treatment is more informative. Already in its initial state its value is less than the table value which according to [23] makes 0.2038 nm, and with the growth of T_a this difference only rises. The observed compression of the lattice along the normal can be interpreted as a reflection of its stretching in the film plane, which, in its turn, may arise from differences in the coefficients of thermal expansion of the film and the substrate.

Magnetic hysteresis is one of the most sensitive indicators of structural and compositional modification. Fig. 2, *a* shows hysteresis loops for Ta/Ni/Ta, measured at different stages of annealing along the axis of the process field application. Their shape suggests that the annealing effect manifests itself in both low-temperature ($T_a = 200\,^\circ$C) and high-temperature ($T_a = 400\,^\circ$C) versions. In the first case, the shape of the loop changes and the coercive force H_c slightly decreases, in the second — there is a fundamental change in the nature of remagnetization, including a fivefold increase of H_c. More detailed information about the changes in hysteresis properties that occur during thermomagnetic treatment can be obtained from the angular dependences of the coercive force $H_c(\varphi)$ shown in Fig. 2, *b*. φ corresponds to the angle in the film plane between the axis of the process field and the axis of remagnetization. As can be seen, for films in the initial state, this dependence is characterized by the presence of two local maxima at angles $\varphi = 0°$ and 90°. This indicates the biaxial character of the magnetic anisotropy in the plane of the films, which, according to [24] is formed as a result of the superposition of two mechanisms reflecting the features of the defective structure of films. On the one hand, it is the magnetostatic mechanism [25], which assumes that there's an anisotropic distribution of defects along the boundaries of crystallites and formation of an easy axis (EA) along the axis of application of the process magnetic field. On the other hand, it is a magnetoelastic mechanism based on the anisotropy of elastic stresses in the plane, which, in its turn, arises from the anisotropy of the defective structure. In case of negative magnetostriction and anisotropic relaxation of tensile elastic stresses, this mechanism gives an EA perpendicular to the process field.

After low-temperature thermomagnetic treatment ($T_a = 200\,^\circ$C), the nature of the anisotropy changes — it actually becomes uniaxial with EA and perpendicular to the axis of application of the process field. This may be the consequence of more intensified tensile elastic stresses (see comment to dependence $h(T_a)$, given in table) which results in the predominance of the magnetic elastic mechanism. At $T_a = 300\,^\circ$C the situation changes again and the dependence $H_c(\varphi)$ becomes looking as initial version. Probably, such thermomagnetic treatment

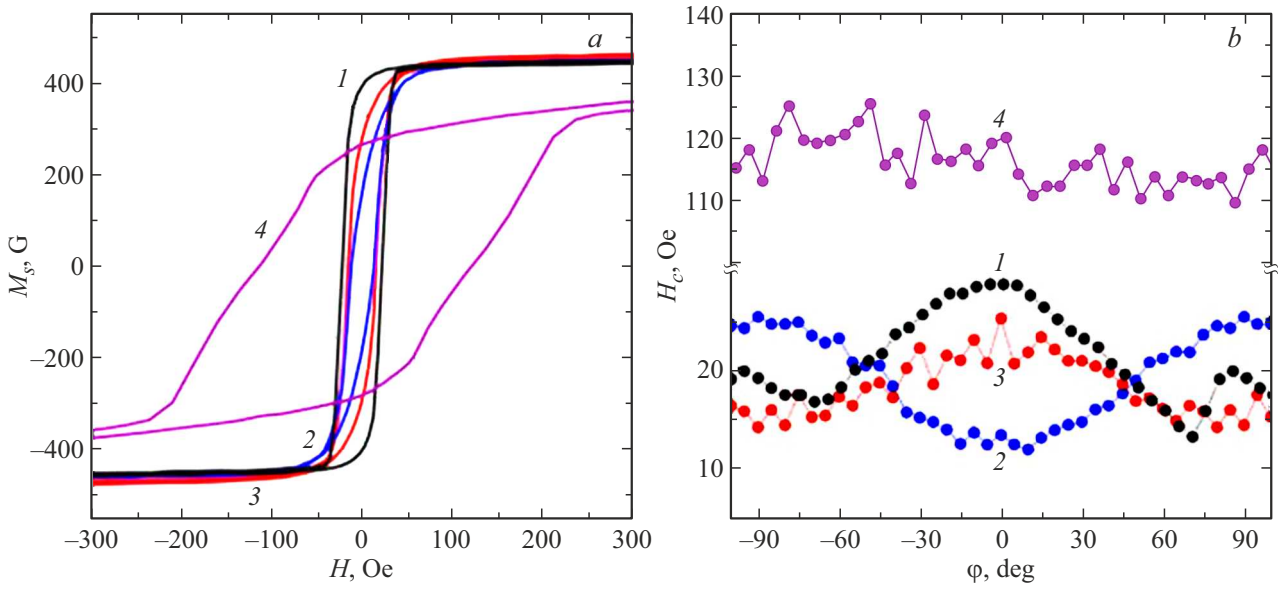

Figure 2. Hysteresis loops measured along the axis of the process field ($\varphi = 0°$) (*a*) and angular dependences of the coercive force of Ta/Ni/Ta films subjected to thermomagnetic treatment at temperatures: *1* — initial state; *2* — 200 °C; *3* — 300 °C; *4* — 400 °C (*b*).

intensified the directed migration of defects, which brought the magnetostatic mechanism to the fore. The given interpretation of the magnetic properties suggests that up to and including $T_a = 300\,^{\circ}\mathrm{C}$, structural transformations are localized directly in Ni layer and are not directly related to the presence of adjacent metal layers. Their factor most likely becomes significant at $T_a = 400\,^{\circ}\mathrm{C}$. As noted above, such annealing leads to a sharp increase in H_c, which can be associated with some interlayer mixing and the formation of Ni–Ta interfaces, characterized by high magnetic hysteresis and preventing the remagnetization of the entire Ni layer. Considering that these interfaces are responsible for the flat sections of the hysteresis loop (curve *4* in Fig. 2, *a*), and taking into account that the saturation magnetization practically does not change during annealing ($M_s = (440 \pm 10)$ G), it is possible to find their thickness. The corresponding estimate shows that, in total, it is about 8 nm on the two surfaces of Ni layer. Note also that the specified value M_s is slightly less than the tabular value for Ni (485 G [26]). But this is typical of thin films, primarily because of the reduced density.

3. Structure and magnetic properties of films Ta/$Fe_{20}Ni_{80}$/FeMn/Ni/Ta

We may judge on the initial structure of Ta/$Fe_{20}Ni_{80}$/FeMn/Ni/Ta films and its changes during thermomagnetic treatment based on the diffraction patterns in Fig. 3, *a*. As can be seen, at $T_a \le 300\,^{\circ}\mathrm{C}$ they all contain two lines identified as a result of reflection from the planes (111) of FCC of FeMn layers lattice (left reflex) and Ni (right reflex). It follows that γ-FeMn layer, which carries antiferromagnetism, is present in the film structure and that it, like the Ni layer, has a strong crystalline texture necessary to create a magnetic bias in the adjacent ferromagnetic layer. The permalloy auxiliary layer is not identified on diffraction patterns, probably due to its small thickness. The quantitative characteristics of the structural state of the layers are presented in the following table. At the same time, the partially overlapping diffraction reflections, which were used to determine the structural parameters, was separated using FullProf Suite software. These data show that at $T_a \le 300\,^{\circ}\mathrm{C}$, the Ni layer in the new environment has greater stability of D and interplane distance h, which is probably inherited from the underlying FeMn layer, which exhibits low sensitivity of these characteristics to annealing. At the same time, judging by the value of h, there are tensile stresses in the plane in Ni layer, as in the previous case. They probably also exist in FeMn layer, since h, although not much, is still below the equilibrium value, which according to [27] is 0.281 nm. The clearly distinct structural changes include annealing at 400 °C. In the diffraction pattern, the line corresponding to γ-FeMn has actually disappeared, but a new reflex has appeared at large diffraction angles; the asymmetry of its shape, as well as the blurring and displacement of Ni line, can be interpreted as the result of nondistinct elementary localization within the entire layered structure. It should also be stressed that there are no lines in the area of the asymmetric reflex corresponding to simple phases such as Fe, Mn, α-FeMn, γ-FeNi.

Magnetometry generally confirms the conclusions made about compositional transformations in the layered structure. This follows from a comparison of the hysteresis loops of Ta/$Fe_{20}Ni_{80}$/FeMn/Ni/Ta sample at different annealing stages, measured along the axis of the process field and shown in Fig. 3, *b*. Up to and including $T_a = 300\,^{\circ}\mathrm{C}$, the

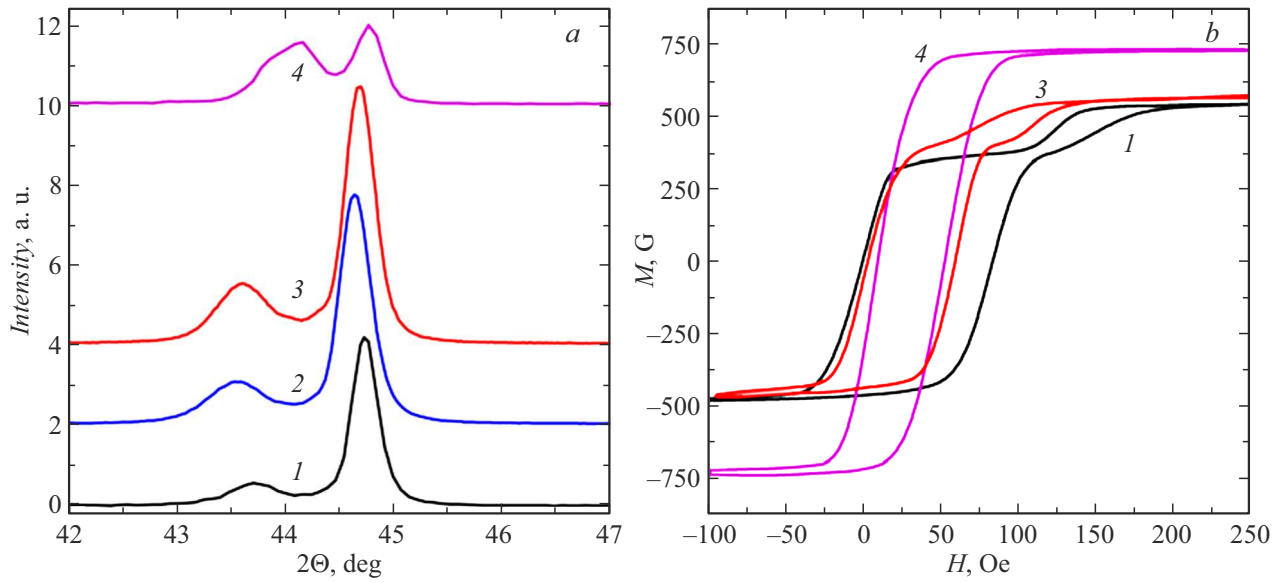

Figure 3. Diffraction patterns (a) and hysteresis loops (b) for Ta/$Fe_{20}Ni_{80}$/FeMn/Ni/Ta sample, measured along the axis of process field after annealing at different temperatures: *1* — initial state; *2* — 200 °C; *3* — 300 °C; *4* — 400 °C.

loops have a two-stage appearance and are offset along the axis of the magnetic field. In fact, they represent themselves the superposition of hysteresis loops of Ni layer (large stage) and the auxiliary permalloy layer (small stage), each of which demonstrates the presence of a magnetic bias realized on different surfaces of the antiferromagnetic layer. Some difference in the span of hysteresis loops of Ni layers in the two types of films may be due to an error in determining the partial thicknesses of the layers, as well as the partial involvement of part of Ni layer in the interlayer ferro-antiferromagnetic interface with a fan-shaped magnetic structure. Annealing at $T_a = 400\,^{\circ}$C leads to a stepless loop with an amplitude greater than that provided by the remagnetization of both ferromagnetic layers at previous stages of thermomagnetic treatment. At that, magnetic bias is still observed. Obviously, the absence of a private loop from the permalloy layer and higher saturation magnetization of the sample can only be associated with compositional transformations and, first of all, in the FeMn layer. Following the authors of [16], it can be assumed that a sublayer rich in Fe with high magnetization is formed in its volume. The experimentally observed increment in the loop span is about 440 G. To ensure it, the thickness of pure α-Fe, if present, should reach at least 6 nm, which is almost a third of the nominal thickness of FeMn layer (20 nm). However, no BCC of iron is observed in the X-ray images. Besides, this experiment does not answer the questions about which composition originated at the site of the initial localization of the permalloy layer and whether Mn diffused into neighboring layers or concentrated within the initial layer, as well as whether Fe and Ni were admixed from the main ferromagnetic layer. Some indirect information on this subject can be found, in particular, in the analysis of Ni layer hysteresis properties.

Fig. 4 illustrates angular dependences of the exchange bias field $H_e(\varphi)$ and coercive force $H_c(\varphi)$. H_e here means the field of the hysteresis loop distance from the zero point, and H_c — denotes the halfwidth of the hysteresis loop. It can be seen that annealing does not qualitatively change the nature of $H_c(\varphi)$ dependencies of Ni layer. At all its stages, the coercive force has a pronounced maximum at $\varphi = 0$, which is typical for media with unidirectional anisotropy. This makes this version of the film structure drastically different from Ta/Ni/Ta films (Fig. 2, b), where the coercive force is sensitive to the nuances of magnetic anisotropy of Ni, which change during annealing. In fact, it is suppressed by an additional and rather strong unidirectional anisotropy. At the same time, after annealing the coercive force changes in quantity. As can be seen, with an increase of T_a, the maximum value of the coercive force decreases by half. And if in the initial state it significantly exceeded the H_c of Ta/Ni/Ta sample, then at $T_a = 300\,^{\circ}$C it reached its level. The reason for the increased hysteresis of the exchange-coupled Ni layer, in particular, may be the presence and change during annealing of an additional component from ultrafine antiferromagnetic FeMn crystallites, which do not contribute to the exchange bias, but increase H_c [28]. We also note the great difference in H_c of the films of two types after annealing at 400 °C. It indirectly confirms the above assumption that the abnormally high coercive force of Ni in the presence of adjacent Ta layers is associated with partial mixing of the layers and the formation of magnetically hard interfaces of Ni−Ta.

In contrast to the coercive force, the angular dependence of the exchange bias field reveals qualitative changes during thermomagnetic treatment. Comparing Fig. 4, b and Fig. 2, b, we can conclude that thermomagnetic

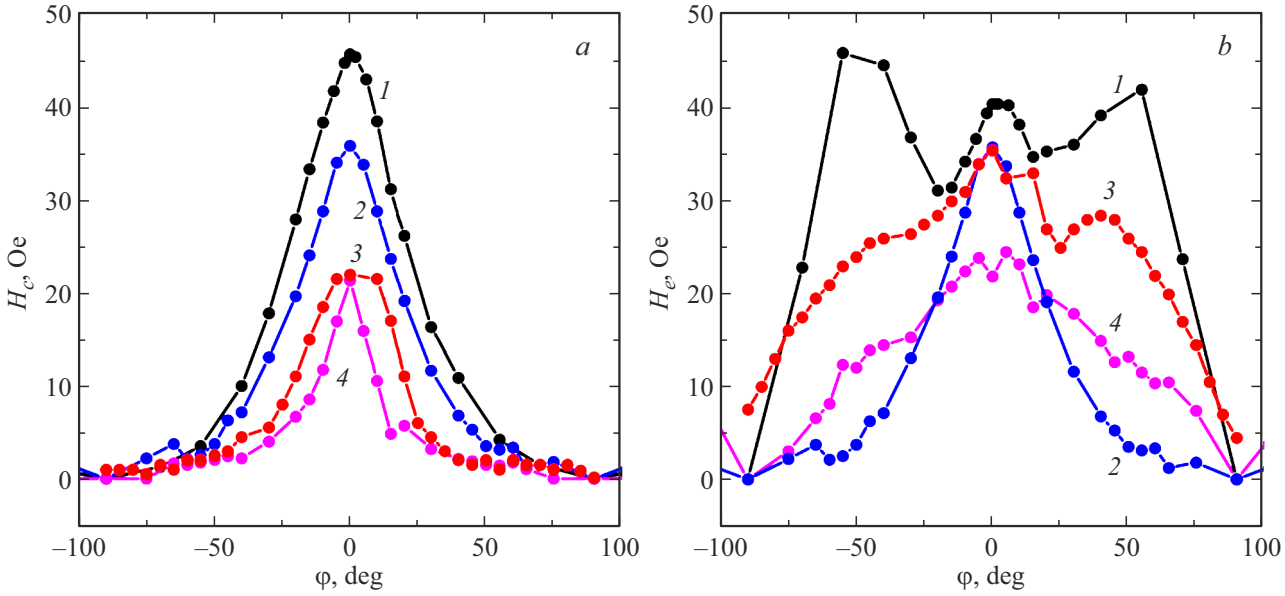

Figure 4. Angular dependences of coercive force (a) and exchange bias field (b) of Ta/$Fe_{20}Ni_{80}$/FeMn/Ni/Ta sample after annealing at different temperatures: *1* — initial state; *2* — 200 °C; *3* — 300 °C; *4* — 400 °C.

treatment has assumed the role of an indicator of the magnetic anisotropy of Ni layer in exchange-bias films. In the initial state, the curve $H_e(\varphi)$ has a rather complex shape, which is significantly simplified at the first step of annealing ($T_a = 200\,^\circ$C), then ($T_a = 300\,^\circ$C) the curve largely restores its path, but in the final version ($T_a = 400\,^\circ$C) again comes to a relatively simple form. In [29], it was shown by simple modeling that the form of $H_e(\varphi)$ strongly depends on the ratio of the values of induced and unidirectional anisotropy and, in particular, dependencies can be realized similar to those illustrated by the curves *1, 3* and *2, 4* in Fig. 4. The analysis of the properties of Ta/Ni/Ta films described above has demonstrated that two mechanisms of induced magnetic anisotropy — magnetostatic and magnetostrictive, probably compete in them, and their role varies depending on the temperature of thermomagnetic treatment, leading to biaxial or uniaxial versions of anisotropy. These changes are most likely reflected in the variations of $H_e(\varphi)$.

4. Elementary analysis of FeMn/Ni profiles

To increase the argumentation base in interpreting the results of studying the structure and magnetic properties of layered films, we conducted a model experiment to directly determine the profiles of the elemental composition of FeMn/Ni samples at different stages of annealing. For this purpose, an X-ray analyzer was used, making possible to change the depth of the layer involved in the formation of the fluorescent signal by precisely varying the angle of incidence of X-ray gazing radiation. This technique, implemented on Nanohunter device, provides reliable information from a depth of no more than 10 nm, which imposed a limit on the thickness of the layers in the model sample (5 nm each).

Fig. 5 shows the dependences of the signal intensities of the fluorescent radiation of Ni, Fe, and Mn elements on the gazing angle of X-ray beam for different annealing stages. For clarity, they are grouped into two pairs of elements Fe–Mn and Ni–Mn, and the curves for $T_a = 200\,^\circ$C are omitted, which differ little from the curves corresponding to the initial state. Note also that measurements in Fe–Mn pair were performed on an X-ray tube with a copper anode, which gives a more intense fluorescent response for these elements, and for Ni–Mn pair — with a molybdenum anode since the first tube does not overlap the fluorescent spectrum Ni. Useful information characterizing the elemental profile of the sample is contained in the relative positioning of the presented curves on the angle scale: the more to the left of the curve, the closer to the surface of the sample lies its forming element. According to this principle, comparing Fig. 5, a and b, it may be concluded that in its initial state Ni lies above Mn, and Fe is located approximately at one depth with Mn, i.e. also below Ni. Thus, the nominal FeMn/Ni structure is reproduced qualitatively correctly.

The low-temperature annealing ($T_a = 200\,^\circ$C) doesn't change the above-mentioned pattern. But at its next step, there is a significant redistribution in the order of the curves of different elements. At $T_a = 300\,^\circ$C, the curves of Mn in both figures took the leftmost position, which was further strengthened after the final annealing. In other words, as a result of annealing, segregation of elements occurred in FeMn layer, and Mn migrated from it through Ni layer to the sample surface. Parallel magnetometry has shown

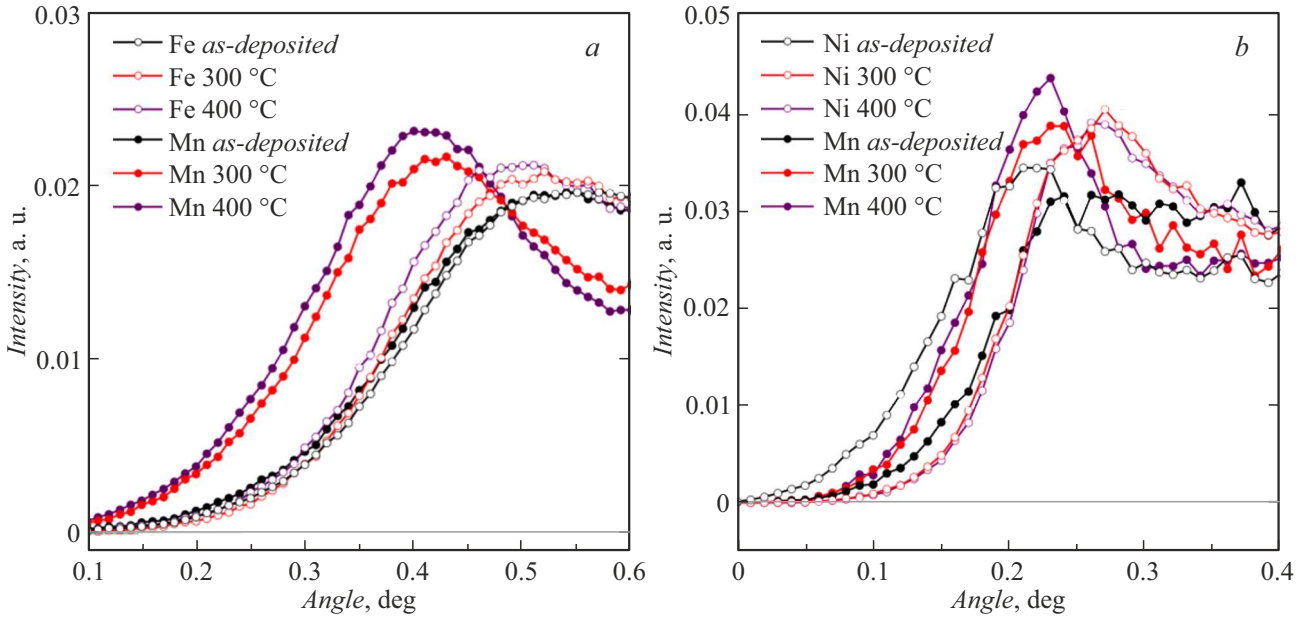

Figure 5. Fluorescent signal versus X-ray beam grazing angle for the elements in FeMn/Ni in pairs Fe−Mn (*a*) and Ni−Mn (*b*) after annealing at different temperatures.

that this redistribution of elements is accompanied by an approximately twofold increase in the magnetic moment of the sample. This confirms the release of Fe, which, judging by the fluorescent curves, can partially mix with Ni, forming a layer of variable composition with an increased magnetic moment.

Of course, the results obtained in this experiment cannot be directly associated with the films with large layer thicknesses. In particular, the Ni reflex is clearly present in the diffraction pattern shown in Fig. 3 after annealing at $T_a = 400\,^{\circ}\mathrm{C}$, although its intensity is significantly lower than at earlier stages of annealing. At the same time, it can be claimed that the greatest effect of high-temperature annealing is a non-uniform elemental diffusion, which spreads deep into the layers by at least 5 nm.

Conclusion

The performed study with the film structures containing Ni layers as examples showed the two-level nature of the thermal effect on the structural and magnetic properties of such objects. When annealing is made at temperatures below 300 °C, the decisive role apparently is played by anisotropy in the distribution of point defects along the crystallite boundary and the tensile stresses formed at the interface of the dielectric substrate−metal film. Their variation leads to a change in the ratio between the magnetostatic and magnetically elastic mechanisms of induced magnetic anisotropy, which is in some specific way effects the anisotropy of the coercive force in Ta/Ni films or the anisotropy of the exchange bias field in FeMn/Ni films. Annealing at high temperatures causes interlayer diffusion, which is confirmed by both measurements of the elemental composition and analysis of magnetic properties. The nature of this diffusion and its effect on the properties of films, as in the case of low-temperature annealing, depend on the type of film structure. In Ta/Ni films, it probably includes only limited delocalization of the layers and formation of a magnetically hard interface, which causes a significant increase in the coercive force of the samples as a whole. In FeMn/Ni films, there is a predominant and significant migration of Mn up to its release onto the surface of the films. This leads to an increase in the magnetically active volume formed by a solid solution of Fe−Ni of a variable thickness composition, which is manifested as a growing resulting magnetization. However, some of Mn remains within FeMn system, ensuring the presence of antiferromagnetism and the associated magnetic bias.

Funding

The study has been funded by the Ministry of Education and Science of Russia, project FEUZ-2024-0060.

Conflict of interest

The authors declare that they have no conflict of interest.

References

[1] D. Sander, S.O. Valenzuela, D. Makarov, C.H. Marrows, E.E. Fullerton, P. Fischer, J. McCord, P. Vavassori, S. Mangin, P. Pirro. J. Phys. D: Appl. Phys., **50**, 36001 (2017). DOI: 10.1088/1361-6463/aa81a1

[2] B. Lim, M. Mahfoud, P.T. Das, T. Jeon, C. Jeon, M. Kim, T.-K. Nguyen, Q.-H. Tran, F. Terki, C.G. Kim. APL Mater., **10**, 051108 (2022). DOI: 10.1063/5.0087311
[3] I. Žutic, J. Fabian, S. Das Sarma. Rev. Mod. Phys., **76**, 323 (2004). DOI: 10.1103/RevModPhys.76.323
[4] G. Khandi. Elektronnye komponenty, **3**, 74 (2018) (in Russian).
[5] K. O'Grady, L.E. Fernandez-Outon, G. Vallejo-Fernandez. J. Magn. Magn. Mater., **322** (8), 883 (2010). DOI: 10.1016/j.jmmm.2009.12.011
[6] K. O'Grady, J. Sinclair, K. Elphick, R. Carpenter, G. Vallejo-Fernandez, M.I.J. Probert, A. Hirohata. J. Appl. Phys., **128** (4), 040901 (2020). DOI: 10.1063/5.0006077
[7] D. Xiong, Y. Jiang, K. Shi, A. Du, Y. Yao, Z. Guo, D. Zhu, K. Cao, S. Peng, W. Cai, D. Zhu, W. Zhao. Fundamental Research, **2** (4), 522 (2022). DOI: 10.1016/j.fmre.2022.03.016
[8] V.O. Vas'kovskiy, V.N. Lepalovskij, A.N. Gorkovenko, N.A. Kulesh, P.A. Savin, A.V. Svalov, E.A. Stepanova, N.N. Shchegoleva, A.A. Yuvchenko. Tech. Phys., **60** (1), 116 (2015). DOI: 10.1134/S1063784215010260
[9] G.V. Anderson, M. Pakala, Y. Huai. IEEE Trans. Magn., **36**, 2605 (2000). DOI: 10.1109/20.908530
[10] M. Takiguchi, S. Ishii, E. Makino, A. Okabe. J. Appl. Phys., **87** (5), 2469 (2000). DOI: 10.1063/1.372204
[11] S.H. Jang, T. Kang, H.J. Kim, K.Y. Kim. J. Appl. Phys. Lett., **81** (1), 105 (2002). DOI: 10.1063/1.1491605
[12] R.-T. Huang, F.-R. Chen, J.-J. Kai, W. Kai, I.-F. Tsu, S. Mao. J. Magn. Magn. Mater., **260** (1−2), 28 (2003). DOI: 10.1016/S0304-8853(01)00458-9
[13] Y.K. Kim, G.-H. Park, S.-R. Lee, S.-H. Min, J.Y. Won, S.A. Song. J. Appl. Phys., **93** (10), 7924 (2003). DOI: 10.1063/1.1540158
[14] J.S. Kim, S.-R. Lee. J. Appl. Phys., **99**, 08R704 (2006). DOI: 10.1063/1.2172200
[15] S.W. Kim, J.K. Kim, J.H. Kim, B.K. Kim, J.Y. Lee, S.S. Lee, D.G. Hwang, J.R. Rhee. J. Appl. Phys., **93** (10), 6602 (2003). DOI: 10.1063/1.1557238
[16] P. Savin, J. Guzmán, V. Lepalovskij, A. Svalov, G. Kurlyandskaya, A. Asenjo, V. Vas'kovskiy, M. Vazquez. J. Magn. Magn. Mater., **402**, 49 (2016). DOI: 10.1016/j.jmmm.2015.11.027
[17] K.G. Balymov, E.V. Kudyukov, V.N. Lepalovsky, N.A. Kulesh, V.O. Vaskovsky. Defektoskopiya **7**, 46 (2017) (in Russian).
[18] K.-Y. Kim, H.-C. Choi, C.-Y. You, J.-S. Lee. J. Appl. Phys., **105**, 07D715 (2009). DOI: 10.1063/1.3068628
[19] N.M. Lyadov, V.V. Bazarov, I.R. Vakhitov, A.I. Gumarov, Sh.Z. Ibragimov, D.M. Kuzina, I.A. Faizrakhmanov, R.I. Khaibullin, V.A. Shustov. Phys. Solid State, **63** (10), 1723 (2021). DOI: 10.1134/S1063783421100231
[20] K.-C. Chen, Y.H. Wu, K.-M. Wu, J.C. Wu, L. Horng. J. Appl. Phys., **101** (9), 09E516 (2007). DOI: 10.1063/1.2712319
[21] P. Scherrer. Nachrichten von der Gesellschaft der Wissenschaften zu Göttingen, Mathematisch-Physikalische Klasse, **2**, 98 (1918).
[22] J. Rodríguez-Carvajal. Phys. B: Condens. Matter., **192** (1−2), 55 (1993). DOI: 10.1016/0921-4526(93)90108-I
[23] N.P. Yurkevich, P.G. Kuzhir, R.L. Tofpenets. *Electronno-microscopicheskoye issledovanie structuri kristallov* (BNTU, Minsk, 2004)
[24] P.A. Savin, O.A. Adanakova, V.N. Lepalovskij, E.V. Kudyukov, V.O. Vas'kovskiy. Bull. RAS: Phys., **87** (4), 433 (2023). DOI: 10.3103/S1062873822701398
[25] A.G. Lesnik. *Induced Magnetic Anisotropy* (Naukova Dumka, Kiev, 1976)
[26] J.M.D. Coey. *Magnetism and Magnetic Materials* (Cambridge University Press., NY., 2010). DOI: 10.1017/CBO9780511845000
[27] M. Ekholm, I.A. Abrikosov. Phys. Rev. B., **84**, 104423 (2011). DOI: 10.1103/PhysRevB.84.104423
[28] V.O. Vaskovsky, A.A. Bykova, A.N. Gorkovenko, M.E. Moskalev, V.N. Lepalovsky. ZhETF **165** (5), 655 (2024) (in Russian). DOI: 10.31857/S0044451024050067
[29] A.N. Gorkovenko, N.A. Kulesh, P.A. Panchenko, V.O. Vaskovskiy. Inorg. Mater. Appl. Res., **11** (1), 172 (2020). DOI: 10.1134/S2075113320010141

Translated by T.Zorina